Efficient implementation of the Hellmann–Feynman theorem in a diffusion Monte Carlo calculation
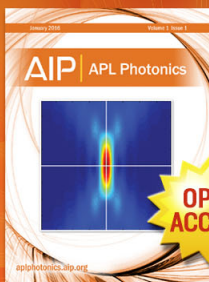
S. A. Vitiello

Articles you may be interested in

Monte Carlo calculation of electron diffusion coefficient in wurtzite indium nitride
Appl. Phys. Lett. **100**, 142105 (2012); 10.1063/1.3700720

Exact ground state Monte Carlo method for Bosons without importance sampling
J. Chem. Phys. **131**, 154108 (2009); 10.1063/1.3247833

Weak intermolecular interactions calculated with diffusion Monte Carlo
J. Chem. Phys. **123**, 184106 (2005); 10.1063/1.2110165

Efficiency considerations in the construction of interpolated potential energy surfaces for the calculation of quantum observables by diffusion Monte Carlo
J. Chem. Phys. **121**, 9844 (2004); 10.1063/1.1756580

Integral Hellmann—Feynman Theorem
J. Chem. Phys. **41**, 2892 (1964); 10.1063/1.1726371

Efficient implementation of the Hellmann–Feynman theorem in a diffusion Monte Carlo calculation

S. A. Vitiello[a)]

*Instituto de Física Gleb Wataghin Universidade Estadual de Campinas-*UNICAMP *13083-859, Campinas, SP, Brazil*

Kinetic and potential energies of systems of ^{4}He atoms in the solid phase are computed at $T = 0$. Results at two densities of the liquid phase are presented as well. Calculations are performed by the multiweight extension to the diffusion Monte Carlo method that allows the application of the Hellmann–Feynman theorem in a robust and efficient way. This is a general method that can be applied in other situations of interest as well. © *2011 American Institute of Physics.* [doi:10.1063/1.3532411]

I. INTRODUCTION

The kinetic energy is an important quantity in the characterization of quantum many-body systems. Knowledge of its properties can improve our understanding of a variety of phenomena, for instance its investigation might clarify some aspects related to high T_C superconductors[1–3] and to superfluidity, both in the context of ultracold atomic gases[4,5] and systems made from helium atoms.[6] The kinetic energy may also present[7] an intriguing behavior at finite temperature. It might be smaller in an interacting system than it is in the corresponding free system.

The kinetic energy and the momentum distribution, of which it is the second moment, depend on the system statistics, i.e., if the particles are fermions or bosons and on how they interact. In the classical systems the momentum distribution is of the Maxwell–Boltzmann form and shows a kinetic energy at a temperature T equal to $3k_BT/2$, where k_B is the Boltzmann's constant. As a consequence these systems are predicted to crystallize at low enough temperatures when the potential energy dominates the total energy.

However, systems made from helium atoms remain in the liquid phase even at absolute zero temperature. It is the zero-point energy contribution to the kinetic energy, present at all temperatures, that prevents the system potential energy to dominate the energetic balance, therefore its crystallization. In most systems the zero-point energy is small when compared to the potential attraction and it does not produce this effect.

A decrease in kinetic energy at a given temperature in systems that obey Bose statistics can be considered as evidence of a condensate development. In those formed from ^{4}He atoms in the liquid phase, it has been observed[6,8–10] that the momentum distribution deviates from the Maxwell–Boltzmann distribution as the temperature is reduced. Below a critical Bose condensation temperature a condensate appears and a macroscopic fraction of the atoms occupies the zero momentum state. As a result there is a reduction of the kinetic energy. An experiment[6] at the equilibrium density reveals that as

the temperature is reduced from 2.3 to 0.5 K, crossing the superfluid critical temperature, the lambda point at $T = 2.17$ K, the kinetic energy decreases by about 10%, viz. 1.8 K. This drop is attributed to the formation of a condensate fraction where approximately 10% of the atoms fill the zero momentum state. Unlike the ideal Bose gas, not all the particles go into the condensate even at zero temperature. The depletion of the condensate can be attributed to the strong interacting character of the ^{4}He systems. The strong short-range interactions originate a kind of spherical cage around each particle. And according to the Heisenberg uncertainty principle they impose constraints on the atoms originating a spread in the occupation probability of any momentum state.

In the solid phase, if the atoms developed a Bose-Einstein condensate (BEC), a similar behavior would be observed. This was predicted to occur long ago. Chester,[11] based on wavefunction models for the ^{4}He solid phase, suggested that vacancies in the ground state would lead to a fraction of the atoms to condense in the zero momentum state. Moreover, according to Leggett,[12] its rotation would be anomalous, just like a superfluid, i.e., a fraction of the solid total mass would decouple from the motion. In 2004, Kim and Chan[13,14] using a torsional oscillator observed a decrease in the oscillation period of a sample of ^{4}He below about 200 mK. This result was interpreted as evidence of nonclassical rotation inertia where approximately 1% of the mass sample became decoupled from the oscillation and accordingly it would characterize supersolidity, a super state of matter.

Supersolidity has received independent confirmations[15–18] in a number of different laboratories. It has also been observed that defects play a rôle in the results.[18] Measurements[19,20] of the elastic properties have also revealed shear modulus anomalies that share with supersolidity the same dependence on the temperature and on the ^{3}He impurity concentration. These anomalies were attributed to dislocations motion and pinning.[20–22] Many experimental efforts have been performed to elucidate the underlying structure of the observed nonclassical rotational inertia. Among these experiments, refinements in measurements[23] of the momentum distribution and kinetic energy have been attempted[24–26] so as to put in evidence the existence of a Bose

---

a)Electronic mail: vitiello@ifi.unicamp.br.

condensate. Its formation below a critical temperature could explain supersolidity in analogy to what happens in the liquid phase. A decrease in the kinetic energy in a situation similar to the liquid phase has not been observed.[25,26] However, since the possible supersolid fraction is only about 1%, its effects are small and hard to observe. Moreover, the lowest temperature where measurements were attempted is 70 mK, and now it seems important to go as low as 20 mK.[19] Additionally, the possible interpretations of the results in the solid phase are more delicate than in the liquid. Although the present view[27,28] does not support vacancies in the solid phase, their existence in the limit of temperatures going to zero has not been completely excluded.[29–33] A gas of vacancies could form a condensate and no kinetic energy decrease below the transition temperature would be observed.

The kinetic energy is also a difficult quantity to compute at least at zero temperature. Diffusion Monte Carlo (DMC) is the standard method to estimate total energies at $T = 0$. However, in its straightforward implementation, there are no estimators for quantities that do not commute with the system Hamiltonian. In this paper, motivated by the interest in precise and accurate evaluations of quantities like the kinetic energy, I present a direct methodology that allows its calculation. This is done by implementing the standard Hellmann–Feynman theorem efficiently in a DMC[34,35] calculation. This approach is an alternative to those methods that sample the "pure" ground-state distribution Ψ_0^2. The implementation is made through the multiweight extension to the DMC method,[36] or for shortness, the multiweight DMC method. This calculation scheme is very easy to understand and implement. Moreover and more important, it opens possibilities of applying the Hellmann–Feynman theorem to some other situations of interest where large systems need to be considered. In Sec. II the method is presented. Specific details of the simulations are given in Sec. III. The Sec. IV presents results, comparisons with path-integral Monte Carlo and experimental values. A confrontation with other methods from the literature is also included. In Sec. V conclusions and final comments are made.

II. METHODS

Systems formed from helium atoms in a simple description[37] relies only on a two-body potential $V(r)$. Frequently it assumes the HFD-B3-FCI1 potential of Aziz *et al.*[38] Following this approach, the Hamiltonian considered in this work is given by

$$H = -\frac{\hbar^2}{2m} \sum_i^N \nabla_i^2 + \sum_{i<j}^N V(r_{ij}). \tag{1}$$

The N atoms kinetic energy depends on the ^{4}He mass m.

The DMC method is the standard method to solve the time dependent Schrödinger. This is accomplished by simulating in imaginary time a corresponding classical diffusion process with a source. It is guided by a trial function ψ_T, that is able to give a meaningful description for the system. Although calculations of a quantity like the total energy is relatively easy, those associated to operators that do not commute with the system Hamiltonian are involved. This

happens because, as the system reaches equilibrium in the simulation, the sampled configurations are from $\Psi_0 \psi_T$.

The Hellmann–Feynman theorem could, in principle, avoid this difficulty. The potential energy E_p of a system can be computed through the substitution $V \rightarrow \lambda V$ and performing a derivative of the total energy E_t with respect to λ

$$E_p = \frac{d}{d\lambda} E_t(\lambda) = \left\langle \psi(\lambda) \left| \frac{d H(\lambda)}{d\lambda} \right| \psi(\lambda) \right\rangle. \tag{2}$$

However, attempts to perform a numerical derivative using independent estimates with appropriate values of λ are also very difficult. This is true especially for large systems where the statistical uncertainties can easily lead to a loss of significance in the final result. Correlated sampling is a well known way of minimizing these difficulties and the multiweight DMC method is able to perform this task in an efficient way.

The main idea of the multiweight DMC method is to use as much as possible a single set of configurations or walkers $\{R_i \equiv (\mathbf{r}_1, \ldots, \mathbf{r}_N)_i\}$ to compute the desired quantities. In this work the interatomic potential is multiplied by three constants $\lambda \equiv 1 - \delta$ with $\delta \equiv \{10^{-4}, 0, -10^{-4}\}$. The total energy of the systems are computed by keeping three different weights associated to each walker. Of course, a total energy corresponding to one of the δ values should agree within statistical uncertainties with the result obtained by the standard application of the DMC method in the equivalent Hamiltonian. In the multiweight DMC, numerical derivatives are carried out and quantities of interest and their standard deviation computed, as usual. Following, I present a brief overview of the multiweight DMC method. An extended description of the multiweight DMC method can be found in Ref. 36.

The drift-diffusion step for a walker is performed exactly as in standard DMC calculations. It depends only on the chosen guiding function. A configuration R' from the old generation goes to the new one R regardless of any weight

$$G_D(R, R') = \frac{e^{-(R-R'-D\Delta\tau\upsilon(R'))^2/(4D\Delta\tau)}}{(4\pi D\Delta\tau)^{3N/2}}, \tag{3}$$

where $D = \hbar/2m$ is a diffusion constant, $\upsilon(R) = 2\nabla \ln \psi_G \times (R)$, and $\Delta\tau$ is the time step.

In the branching step each one of the three weights attached to the walker R' are independently updated. The weight $w_{R'}$ associated to a particular value of the amplitude λ is refreshed according the usual prescription

$$w_R^\lambda = w_{R'}^\lambda G_b^\lambda(R, R'), \tag{4}$$

where

$$G_b^\lambda(R, R') = e^{-\left(\left(E_L^\lambda(R)+E_L^\lambda(R')\right)/2 - E_T^\lambda\right)\Delta\tau} \tag{5}$$

and $E_L^\lambda = H(\lambda)\psi_G/\psi_G$ is the local energy for the Hamiltonians $H(\lambda)$; the E_T^λ are the respective trail energies.

It is important to observe that for a given set of walkers it is impossible to distinguish the updates described above from those that could be made through three standard DMC calculations with Hamiltonians $H(\lambda)$. There are three weights associated to a walker i, (w_i^+, w_i^0, w_i^-), respectively for $\delta = (10^{-4}, 0, -10^{-4})$.

For efficiency reasons branching rules need to be applied. Since in the multiweight DMC there are three weights

attached to each walker and not just one as in the standard DMC, the branching rules need to be generalized. However, this is made in a way that the results for the total energy obtained with Hamiltonians $H(\lambda)$ would agree with three independent runs made with a standard DMC implementation for these Hamiltonians. The generalized branching rules are in fact the only real addition introduced by the multiweight DMC method into the standard calculation.

The generalizations made are quite simple, specially in the cases where walkers do not need to be combined. First, suppose that all weights of a walker are greater than two. In this case it is split in two copies, each one carrying one half of the original weights. This step may be repeated if needed. The second case where the generalization is immediate is when at least one of the attached weights has a value between the threshold w_{thr} and two. In this case just keep the walker with its weights.

In fact the combination of walkers that have all weights smaller than w_{thr} is also simple. Let us assume that the walker R_i is in this situation. In this case it is put aside. If a second walker R_j satisfying this condition appears, the pair of walkers (R_i, R_j) needs to be combined. Eventually one of them will be deleted if all of its weights become zero. The combination rule considers each pair of weights (w_i, w_j) independently. There are three pairs of weight to be considered, (w_i^+, w_j^+), (w_i^0, w_j^0), and (w_i^-, w_j^-). The usual combination rule is applied

(1) For $(\cdot)$ in $\{+, 0, -\}$ compute $w_{sum} = w_i^{(\cdot)} + w_j^{(\cdot)}$.
(2) If $w_{sum} = 0$, keep for both walkers the value zero for this particular weight, and compute the next one, step (1),
(3) else with probability $w_i^{(\cdot)}/w_{sum}$ assign to configuration R_i the weight w_{sum} and zero to R_j, otherwise zero is assigned to R_i and w_{sum} to R_j. If the set $\{+, 0, -\}$ has not been exhausted go to step (1).
(4) Delete a walker if and only if all its attached weights are zero.

After all weights have been updated and the generation has been completed, a new one starts.

Of course, a given walker with two or only one of its weights different from zero contributes only in the estimation of the energies associated to these nonzero weights. It is important to keep these walkers because we want this method to be strictly equivalent to a regular DMC calculation. In other words, the results obtained either by the multiweight DMC or by the standard method for a given Hamiltonian should agree within statistical uncertainties. Although this kind of walker destroys the correlated sampling we want to build, this situation can be easily managed. First of all, by properly choosing the value of w_{thr} the fraction of this kind of walkers can be made small enough. Second, if a walker reaches the point of having one or two weights equal to zero, the remaining nonzero weights will be quite small. Finally, walkers of this kind, in the next generation, are strong candidates to enter into the process where they need to be combined because of the small weights they already have, which can lead to a further reduction of their number.

A threshold weight $w_{thr} = 0.3$ produced only a small fraction of uncorrelated walkers. Certainly this fraction also

depends on the potential amplitude λ in the Hamiltonians $H(\lambda)$. In another kind of calculation with the multiweight DMC method, different interatomic potentials having well depths differing by more than 0.1 K were compared, and in that case less than 5% (Ref. 37) of the walkers have one or two of their weights equal to zero. In this work, as the Hamiltonians differ from each other by a factor of 10^{-4} in the potential amplitude, the issue of how many walkers have weights equal to zero should raise less concern. Of course, since the multiweight DMC is doing no more than use a single set of walkers to estimate energies of three slightly different Hamiltonians, the known difficulties and their possible remedies for DMC calculations can also be applied here. In particular it is necessary to take into account[39] correlations of the walkers both in time and among themselves, since in long runs there is always the possibility that all of them have a single ancestor, a situation that would imply a loss of statistical accuracy.

Following a common practice, the detailed balance condition is restored in the short time approximation of the Green's function by introducing an accept–reject step.[35] Accordingly, an effective time step was considered in the calculations to take into account the rejection of some moves. In this manner somewhat smaller fluctuations resulted.

As usual, the length of the simulation is divided into blocks. For each one, the total energy for the values of the multiplicative factor λ of the potential is computed. These estimates in a block α, E_α^+ and E_α^-, are then used to evaluate the potential energy

$$V_\alpha = \frac{E_\alpha^+ - E_\alpha^-}{2\delta}. \tag{6}$$

The kinetic energy is immediately obtained through E_α^0, the total energy computed for the Hamiltonian $H(\lambda = 1)$

$$T_\alpha = E_\alpha^0 - V_\alpha. \tag{7}$$

Standard errors of all quantities were determined by the usual statistical treatment.

III. COMPUTATIONAL DETAILS

The guiding function used in the calculations were the simplest possible. In the liquid phase it was a function of the Jastrow form with a McMillan pseudopotential

$$\psi_J(R) = \prod_{i<j} e^{-\left(\frac{b}{r_{ij}}\right)^5}. \tag{8}$$

In the solid phase the guiding function was of the Nosanow–Jastrow form. It is given by a product of one-body localization factors of the atoms around sites of a chosen lattice $\mathbf{l}_i$, multiplied by the Jastrow factor that includes pairwise correlation terms

$$\psi_{NJ}(R) = \psi_J(R) \prod_i e^{-\frac{C}{2}|\mathbf{r}_i - \mathbf{l}_i|^2}. \tag{9}$$

Although these are the simplest meaningful guiding functions that can be used, the one employed in the solid phase has an important limitation. It does not support the existence of a Bose–Einstein condensate of atoms.[40] This fact has not precluded its use in the investigation of many properties of the

systems formed from helium atoms along the years.[41,42] To show that calculations of the kinetic energy in large systems are feasible, using the multiweight DMC method for a direct implementation of the Feynman–Hellmann theorem, the Nosanow–Jastrow wave function can safely be used.

Initial configurations for a multiweight DMC calculations were drawn from the guiding functions squared. Variational Monte Carlo runs were made to determine the optimal values of the b and C parameters. The calculations begin with filtering of excited states considering only the actual interatomic potential $V(r)$. The equilibration was completed by considering further steps using the multiweight methodology. After this, accumulation of the quantities of interest started.

Runs were performed for systems of 180 bodies starting from a hcp lattice structure. Extrapolation of $\Delta\tau \to 0$ was unnecessary because the acceptance during all runs were kept at a level of 99% and already contemplate the extrapolate values. A typical population was about 1100 walkers. This number of walkers did not fluctuate in a run by more than 8%. The trial energy was automatically updated about each 40 generations and changed only about 1% during the whole length of the calculation. With this setup, kinetic, potential, and total energies of systems formed from ^{4}He atoms were computed at five densities in the solid phase. In the liquid phase it was computed near the freezing and equilibrium densities.

The convergence of the total energy was easily verified by following its behavior along the blocks in which a run length was divided. The kinetic and potential energies were readily computed through Eqs. (6) and (7), after they have converged. Their convergence was also followed by examining how their values evolved during the simulation.

IV. RESULTS AND DISCUSSION

The kinetic, potential, and total energies of systems formed from ^{4}He atoms in the solid phase were computed using the HFD-B3-FCI1 (Ref. 38) interatomic potential at several densities. At $\rho = 30.60$ nm^{-3} these quantities were computed also with a different potential, HFDHE2.[43] This was done mainly for testing the internal consistency of the calculations, but also for comparison purposes with other calculations. The obtained results are presented in Table I.

TABLE I. Kinetic, potential, and total energies in degrees K per ^{4}He atom at the given densities ρ. The (*) marked density indicates a calculation made with the HFDHE2 potential.

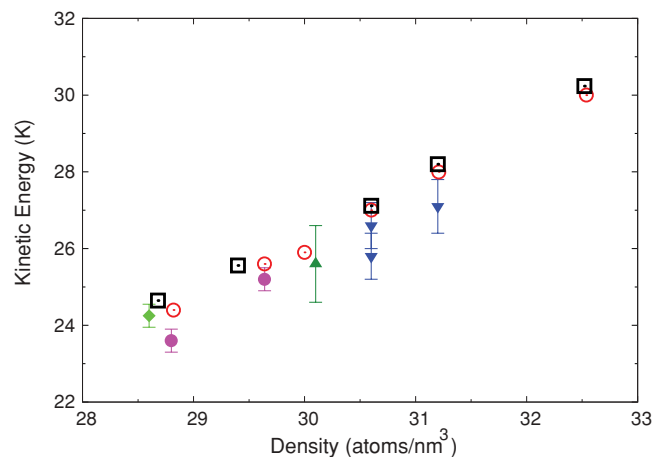| ρ (nm^{-3})	T	V	E
	Solid		
28.68	24.664 ± 0.092	-30.736 ± 0.088	-6.072 ± 0.011
29.40	25.559 ± 0.069	-31.439 ± 0.072	-5.880 ± 0.006
30.60	27.116 ± 0.062	-32.419 ± 0.066	-5.302 ± 0.012
30.60*	27.092 ± 0.068	-32.333 ± 0.062	-5.240 ± 0.009
31.20	28.20 ± 0.10	-33.523 ± 0.099	-5.320 ± 0.014
31.52	30.234 ± 0.061	-34.910 ± 0.072	-4.676 ± 0.014
	Liquid		
21.86	14.472 ± 0.099	-21.618 ± 0.094	-7.145 ± 0.011
25.93	18.65 ± 0.15	-25.06 ± 0.16	-6.403 ± 0.017

FIG. 1. Kinetic energy E_k as a function of density ρ. Results from this work are depicted by open squares (□). Open circles (○) show PIMC results from Refs. 44 and 45. Filled symbols stand for experimental data (◆, ●, ▲, ▼) from Refs. 23, 25, 26, and 44, respectively. Where error bars are not visible they are smaller than the symbol size.

Comparisons of the computed kinetic energies with experimental data[23,25,26,44] and results from path-integral Monte Carlo[44,45] are made in Fig. 1.

The agreement between results obtained in this work and by path-integral Monte Carlo is excellent. Moreover both are in agreement with the experimental data within statistic uncertainties. However since the theoretical results are not scattered above and below the experimental data, this might suggest that the simulations are systematically overestimating values from experiments. Is this situation due to an inadequacy of the guiding function? The Nosanow–Jastrow wave function used for this purpose, as it was mentioned following Eq. (9), is not able to describe a BEC that might exist at $T = 0$. In this context it would be interesting to perform a more detailed study of size effects. The tail correction for the potential energy, most probably, is canceled out when the numeric derivative needed by the Hellmann–Feynman theorem is performed. However, the simple approach of assuming the pair distribution function equal to one, beyond half the smallest side of the simulation cell with 180 bodies, might not be adequate for the total energy calculation and, therefore, of the kinetic energy, because of Eq. (7).

The results obtained with the interatomic potential HFDHE2 at $\rho = 30.60$ nm^{-3} are presented in Table. I. The comparison with the results determined with the HFD-B3-FCI1 potential, also displayed in this table, shows that the kinetic energy obtained with these two potentials cannot be distinguished within statistical uncertainties. It is interesting and nontrivial that different interatomic potentials do not imply change in the kinetic energy, even if the total energies change by a small but significant amount.

The kinetic, potential, and total energies were estimated at the ^{4}He liquid phase near the freezing and equilibrium densities, $\rho = 25.96$ nm^{-3} and 21.86 nm^{-3}, respectively.[46] The kinetic energy at $\rho = 21.86$ nm^{-3} is in excellent agreement within statistical uncertainties with the experimental value[6] 14.45 ± 0.3 K measured at saturated vapor pressure and $T = 0.5$ K. This total energy is about 0.1 K lower than a

previous result[42] obtained using the Green's function Monte Carlo method. A possible source of this discrepancy might be size effects, since in that work only 108 bodies were considered. Below the lambda transition, at the freezing density, it seems that the kinetic energy has not been experimentally measured.

It is worthwhile to compare this method, where the kinetic energy is estimated by the standard Hellmann–Feynman theorem implemented in a multi–weight DMC calculation, with others from the literature. Along the years several approaches have been developed to deal with the fact that in its direct implementation the DMC method does not provide a way of estimating quantities that do not commute with the system Hamiltonian. The most used one, the so-called mixed estimation,[47,48] uses variational estimates of the quantities of interest to obtain their "exact" values. However, they do not always have the required accuracy,[36] because of their dependence on approximated results.

For local operators one of the first attempts to avoid this limitation is known as forward walking.[49,50] It recovers the right estimates by tagging the walkers and keeping track of the asymptotic population. However, this technique is not well behaved for large systems and with poor trial functions. Further developments that try to avoid large fluctuations introduced by the asymptotic offspring have also been proposed.[51] Related to this method there is one known as time correlation,[52] where by generalizing the Fermion transient method pure ground-state averages can be computed. Assaraf and Caffarel[53] have proposed to compute forces in DMC by using the Hellmann–Feynman theorem. They apply a generalized zero-variance property for any observable to obtain finite variance for the estimator, accomplished by the renormalization of the force expression. The reptation method[54] in addition to the asymptotic distribution generated by the simulation of Schrödinger's equation in imaginary time considers other properties of this classical diffusion process. The common ground of all methods is the need of computing new weights either explicitly or by random walks. In some of them it is also necessary to tag the walkers and their offspring. As a result they can be computationally very expensive. Moreover it is unclear how they behave when large systems are considered.[55–57]

On the other hand, calculations performed applying the multiweight DMC in the direct implementation of the Hellmann–Feynman theorem are straightforward. It is also possible to say that the computational effort to estimate the kinetic and potential energies represent only a little overhead of a basic calculation, cf. the Methods section.

V. CONCLUSIONS

The Hellmann–Feynman theorem can be applied in a robust and easy way to compute the kinetic and potential energies using the multiweight diffusion Monte Carlo method. For the systems formed from ^{4}He atoms in the liquid phase and near the freezing density the estimated kinetic energy is in excellent agreement with the experiment. As discussed, the experimental data of this quantity in the solid phase might be slightly overestimated in the simulations. For instance,

consider the situation near the lowest density where the kinetic energy has been estimated, $\rho = 28.68$ nm^{-3}. The experimental value 24.25 ± 0.3 K measured at a slightly low density $\rho = 28.6$ nm^{-3} is about 1.6% lower than the theoretical estimate. The reasons why the agreement between experimental and theoretical values in the liquid phase is better than those in the solid are open questions. Maybe a refined guiding function[32] that supports the existence of a BEC could give additional clues to elucidate this point.

The method I have presented to compute kinetic and potential energies is very general. It is easy to implement and test. Each total energy determined using this approach must agree within statistical uncertainties with results obtained in a regular calculation with the DMC method for the correspondent potential. Moreover the same ideas with straightforward modifications can be applied to some of the situations where the application of the Hellmann–Feynman theorem can be useful.

[1] A. D. LaForge, W. J. Padilla, K. S. Burch, Z. Q. Li, A. A. Schafgans, K. Segawa, Y. Ando, and D. N. Basov, Phys. Rev. Lett. **101**, 097008 (2008).
[2] S. Chakravarty, H.-Y. Kee, and E. Abrahams, Phys. Rev. Lett. **82**, 2366 (1999).
[3] J. E. Hirsch, Phys. Rev. Lett. **59**, 228 (1987).
[4] C. A. Regal, M. Greiner, S. Giorgini, M. Holland, and D. S. Jin, Phys. Rev. Lett. **95**, 250404 (2005).
[5] C. A. Regal, C. Ticknor, J. L. Bohn, and D. S. Jin, Nature (London) **424**, 47 (2003).
[6] H. R. Glyde, R. T. Azuah, and W. G. Stirling, Phys. Rev. B **62**, 14337 (2000).
[7] B. Militzer and E. L. Pollock, Phys. Rev. Lett. **89**, 280401 (2002).
[8] J. Mayers, F. Albergamo, and D. Timms, Physica B **276–278**, 811 (2000).
[9] R. T. Azuah, W. G. Stirling, H. R. Glyde, M. Boninsegni, P. E. Sokol, and S. M. Bennington, Phys. Rev. B **56**, 14620 (1997).
[10] J. Mayers, C. Andreani, and D. Colognesi, J. Phys.: Condens. Matter **9**, 10639 (1997).
[11] G. V. Chester, Phys. Rev. A **2**, 256 (1970).
[12] A. J. Leggett, Phys. Rev. Lett. **25**, 1543 (1970).
[13] E. Kim and M. H.W. Chan, Nature (London) **427**, 225 (2004).
[14] E. Kim and M. H.W. Chan, Science **305**, 1941 (2004).
[15] Y. Aoki, J. C. Graves, and H. Kojima, Phys. Rev. Lett. **99**, 15301 (2007).
[16] A. Penzev, Y. Yasuta, and M. Kubota, J. Low Temp. Phys. **148**, 677 (2007).
[17] M. Kondo, S. Takada, Y. Shibayama, and K. Shirahama, J. Low Temp. Phys. **148**, 695 (2007).
[18] A. S.C. Rittner and J. D. Reppy, Phys. Rev. Lett. **97**, 65301 (2006).
[19] X. Rojas, A. Haziot, V. Bapst, S. Balibar, and H. J. Maris, Phys. Rev. Lett. **105**, 145302 (2010).
[20] J. Day and J. Beamish, Nature (London) **450**, 853 (2007).
[21] D. Aleinikava, E. Dedits, A. B. Kuklov, and D. Schmeltzer, EPL **89**, 46002 (2010).
[22] R. Pessoa, S. A. Vitiello, and M. de Koning, Phys. Rev. Lett. **104**, 085301 (2010).
[23] S. O. Diallo, J. V. Pearce, R. T. Azuah, and H. R. Glyde, Phys. Rev. Lett. **93**, 075301 (2004).
[24] S. O. Diallo, R. T. Azuah, O. Kirichek, J. W. Taylor, and H. R. Glyde, Phys. Rev. B **80**, 60504 (2009).
[25] S. O. Diallo, J. V. Pearce, R. T. Azuah, O. Kirichek, J. W. Taylor, and H. R. Glyde, Phys. Rev. Lett. **98**, 05301 (2007).

[26]M. A. Adams, J. Mayers, O. Kirichek, and R. B.E. Down, Phys. Rev. Lett. **98**, 85301 (2007).

[27]N. Prokof'ev and B. Svistunov, Phys. Rev. Lett. **94**, 155302 (2005).

[28]D. M. Ceperley and B. Bernu, Phys. Rev. Lett. **93**, 55303 (2004).

[29]R. Simmons and R. Blasdell, Precise neutron diffraction study of hcp and bcc ^{4}He, APS March Meeting, Denver, Colorado, Bull. Am. Phys. Soc. **52**, 1 (2007).

[30]P. W. Anderson, Science **324**, 631 (2009).

[31]R. Pessoa, M. de Koning, and S. A. Vitiello, Phys. Rev. B **80**, 72302 (2009)

[32]C. Cazorla, G. E. Astrakharchik, J. Casulleras, and J. Boronat, New J. Phys. **11**, 013047 (2009).

[33]M. Rossi, E. Vitali, D. Galli, and L. Reatto, J. Low Temp. Phys. **153**, 250 (2008).

[34]J. W. Moskowitz, K. E. Schmidt, M. A. Lee, and M. H. Kalos, J. Chem. Phys. **77**, 349 (1982).

[35]P. J. Reynolds, D. M. Ceperley, B. J. Alder, and W. A. Lester, J. Chem. Phys. **77**, 5593 (1982).

[36]S. Ujevic and S. A. Vitiello, J. Chem. Phys. **119**, 8482 (2003).

[37]S. Ujevic and S. A. Vitiello, Phys. Rev. B **71**, 24518 (2005).

[38]R. A. Aziz, A. R. Janzen, and M. R. Moldover, Phys. Rev. Lett. **74**, 1586 (1995).

[39]N. Cerf and O. C. Martin, Int. J. Mod. Phys. C **6**, 693 (1995).

[40]M. Schwartz, Phys. Rev. B **12**, 3725 (1975).

[41]J.-P. Hansen and D. Levesque, Phys. Rev. **165**, 293 (1968).

[42]S. A. Vitiello and K. E. Schmidt, Phys. Rev. B **60**, 12342 (1999).

[43]R. A. Aziz, V. P.S. Nain, J. S. Carley, W. L. Taylor, and G. T. McConville, J. Chem. Phys. **70**, 4330 (1979).

[44]R. C. Blasdell, D. M. Ceperley, and R. O. Simmons, Z. Naturforsch. **48A**, 433 (1993).

[45]D. M. Ceperley, Rev. Mod. Phys. **67**, 279 (1995).

[46]S. Ujevic and S. A. Vitiello, Phys. Rev. B **73**, 12511 (2006).

[47]P. A. Whitlock, D. M. Ceperley, G. V. Chester, and M. H. Kalos, Phys. Rev. B **19**, 5598 (1979).

[48]D. M. Ceperley and M. H. Kalos, *Monte Carlo methods in statistics physics*, 2nd ed. (Springer-Verlag, Berlin, 1986) Chap. Quantum Many-Body Problems, pp. 145–194.

[49]K. S. Liu, M. H. Kalos, and G. V. Chester, Phys. Rev. A **10**, 303 (1974).

[50]R. Barnett, P. Reynolds, and W. A. Lester, Jr., J. Comput. Phys. **96**, 258 (1991).

[51]J. Casulleras and J. Boronat, Phys. Rev. B **52**, 3654 (1995).

[52]D. M. Ceperley and B. Bernu, J. Chem. Phys. **89**, 6316 (1988).

[53]R. Assaraf and M. Caffarel, J. Chem. Phys. **113**, 4028 (2000).

[54]S. Baroni and S. Moroni, Phys. Rev. Lett. **82**, 4745 (1999).

[55]R. J. Needs, M. D. Towler, N. D. Drummond, and P. L. Ros, J. Phys. Condens. Matter **22**, 023201 (2010).

[56]M. D. Towler, Phys. Status Solidi B **243**, 2573 (2006).

[57]G. L. Warren and R. J. Hinde, Phys. Rev. E **73**, 056706 (2006).